AD-767 427

PICOSECOND LASER PULSES

William H. Glenn

United Aircraft Research Laboratories

Prepared for:

Office of Naval Research
Advanced Research Projects Agency

30 September 1973

AD 767427

United Aircraft Research Laboratories

September 24, 1973

Director
Advanced Research Projects Agency
DODAAD CODE HX1241
1400 Wilson Boulevard
Arlington, Virginia 22209

Attention: Program Management

Subject: Semi-Annual Technical Report for Contract N00014-66-C-0344 For the Period 1 March 1973 to 31 August 1973.

Reference: (A) Modification P00012 to the subject contract, effective date, 31 July 1973.

Enclosures: (A) Three (3) copies of United Aircraft Research Laboratories Report M 920479-42

Gentlemen:

In accordance with the provisions of the above modification of the contract (Reference A), we have enclosed three (3) copies of United Aircraft Research Laboratories Report M 920479-42, Enclosure (A). Additional copies of this report have been distributed to the addressees on the attached distribution list.

Very truly yours,

UNITED AIRCRAFT CORPORATION
Research Laboratories

Anthony J. DeMaria

Anthony J. DeMaria
Chief Physicist
Electromagnetics Laboratories

WHG:mk

R

Unclassified

Security Classification

DOCUMENT CONTROL DATA - R&D		
(Security classification of title, body of abstract and indexing annotation must be entered when the overall report is classified)		
1 ORIGINATING ACTIVITY *(Corporate author)* United Aircraft Research Laboratories Silver Land East Hartford, Connecticut 06108	2a REPORT SECURITY CLASSIFICATION Unclassified 2b GROUP	
3 REPORT TITLE Picosecond Laser Pulses		
4 DESCRIPTIVE NOTES *(Type of report and inclusive dates)* Technical, Semi-Annual 1 March 1973 to 31 August 1973		
5 AUTHOR(S) *(Last name, first name, initial)* Glenn, William H.		
6 REPORT DATE 30 September 1973	7a TOTAL NO. OF PAGES 44	7b NO. OF REFS
8a CONTRACT OR GRANT NO N00014-66-C0344 b PROJECT NO c d	9a ORIGINATOR'S REPORT NUMBER(S) M920479-42 9b OTHER REPORT NO(S) *(Any other numbers that may be assigned this report)*	
10 AVAILABILITY/LIMITATION NOTICES		
11 SUPPLEMENTARY NOTES Details of illustrations in this document may be better studied on microfiche.	12. SPONSORING MILITARY ACTIVITY ARPA	

13 ABSTRACT

This contract has been concerned with the application of ultrashort optical pulses to high resolution imaging optical radar. Previous work has demonstrated two dimensional range-doppler imaging of a laboratory target. This was accomplished by range gating the returned signal with a short duration local oscillator pulse. This technique is capable of extremely high time resolution, but it suffers from the problem of inefficient use of the received signal energy. An alternate signal processing technique involving frequency domain sampling has been discussed briefly in the previous semiannual report. During this period further generalization of this scheme has been carried out. This scheme is considerably more versatile than the initial description indicated; it is capable of performing several very useful signal processing operations. It can perform a time scaling on repetitive ultrafast optical signal and stretch its time duration to any desired duration while retaining the functional form of the signal. In addition, it can synthesize an optical match filter for an arbitrary signal. Both of these operations can be performed with electronics that are much slower than the time scale of the original signal.

This report reviews breifly the application of ultrashort pulses to imaging radars, and shows the need for an alternate signal processing scheme. A mathematical description and physical interpretation of frequency domain sampling is

DD FORM 1 JAN 64 1473

Unclassified

Security Classification

Unclassified

Security Classification

14 KEY WORDS	LINK A ROLE	LINK A WT	LINK B ROLE	LINK B WT	LINK C ROLE	LINK C WT
Picosecond Laser Pulses Optical Radar Synthetic Aperture Radar						

ABSTRACT Cont'd

presented and its application to time scaling and matched filtering is discussed. An experiment to demonstrate the technique is outlined and will be carried out during the next reporting period.

ii

UNITED AIRCRAFT CORPORATION
RESEARCH LABORATORIES

Report Number: M-920479-42
Semi-Annual Technical Report for the Period
1 March to 31 August 1973

PICOSECOND LASER PULSES

ARPA Order No.	1806 AMEND #9/11-15-72
Program Code:	3E90
Contractor:	United Aircraft Research Laboratories
Effective Date of Contract:	1 August 1966
Contract Expiration Date:	1 March 1974
Amount of Contract:	$581,628
Contract Number:	N00014-66-C-0-344
Principal Investigator:	Dr. William H. Glenn (203) 565-5411
Scientific Officer:	Dr. Robert E. Behringer
Short Title:	Picosecond Laser Pulses
Reported by:	W. H. Glenn

The views and conclusions contained in this document are those of the author and should not be interpreted as necessarily representing the official policies, either expressed or implied, of the Advanced Research Projects Agency or the U. S. Government.

Sponsored By
Advanced Research Projects Agency
ARPA Order No. 1806

United Aircraft Research Laboratories
Semi-Annual Report M-920479-42
For The Period 1 March 1973 to 31 August 1973

TABLE OF CONTENTS

TECHNICAL REPORT SUMMARY

This contract has been concerned with the application of ultrashort optical pulses to high resolution imaging optical radar. Previous work has demonstrated two dimensional range-doppler imaging of a laboratory target. This was accomplished by range gating the returned signal with a short duration local oscillator pulse. This technique is capable of extremely high time resolution, but it suffers from the problem of inefficient use of the received signal energy. An alternate signal processing technique involving frequency domain sampling has been discussed briefly in the previous semiannual report. During this period further generalization of this scheme has been carried out. This scheme is considerably more versatile than the initial description indicated; it is capable of performing several very useful signal processing operations. It can perform a time scaling on repetitive ultrafast optical signal and stretch its time duration to any desired duration while retaining the functional form of the signal. In addition, it can synthesize an optical matched filter for an arbitrary signal. Both of these operations can be performed with electronics that are much slower than the time scale of the original signal.

This report reviews briefly the application of ultrashort pulses to imaging radars, and shows the need for an alternate signal processing scheme. A mathematical description and physical interpretation of frequency domain sampling is presented and its application to time scaling and matched filtering is discussed. An experiment to demonstrate the technique is outlined and will be carried out during the next reporting period.

SECTION 1

IMAGING OPTICAL RADARS

This contract has been concerned with the application of extremely short duration optical pulses to imaging radars. The problem that has been considered is that of imaging a target whose size and distance is such that it cannot be resolved by conventional optical imaging. If there is relative motion between the target and the radar transmitter, range-doppler processing of the received signal may be used to generate a two dimensional image of the target. The situation is illustrated schematically in Figure 1a. The target is taken to be a collection of scattering centers that are rotating as a rigid body about an axis of rotation. If the received energy is analyzed in time and frequency, a range-doppler image of the target may be constructed as shown in Figure 1b. The contours of constant range are lines perpendicular to the line-of-sight between the transmitter and the target, while the contours of constant doppler shift are parallel to the line of sight. Together, they impose a coordinate system on the target which is used to generate the image. In this simplified case, the image looks exactly like the target. For more complicated, three dimensional targets, the situation is more complicated, but the range-doppler image still gives the projection of the target on the down-range and cross-range directions.

The solution in the down-range direction is determined by the time resolution of the radar; i.e., by the reciprocal of the bandwidth of the transmitted waveform. If the bandwidth is B, then

$$\Delta x = \frac{c}{2B}$$

The resolution in the cross range direction depends on how well the doppler frequencies can be resolved. The doppler shift for a scatterer located at position y is

$$\omega_d = \frac{2\omega v}{c} = \frac{2\omega\Omega y}{c}$$

where Ω is the rotation rate and ω is the optical frequency. If the target is observed for a time τ, then the minimum resolvable doppler shift is $\delta\omega \approx 2\pi/t$. We have then

$$\frac{2\omega\Omega}{c}\ \Delta y > \frac{2\pi}{t}$$

$$\Delta y > \frac{2\pi c}{2\omega\Omega t} = \frac{\lambda}{2\Delta\theta}$$

where $\theta = \Omega t$ is the angle through which the target has turned in the time T. Both Δx and Δy are independent of the range of the target in contrast to the resolution of a conventional imaging system where the minimum resolvable element size increases linearly with range. The magnitude of the doppler shift is

$$\omega_d = \frac{4\pi y \Omega}{\lambda}$$

For a target size of 1 meter

$$\omega_d = 4\pi \times 10^6 \Omega \text{ at } \lambda = 1.06\,\mu$$
$$= 4\pi \times 10^5 \Omega \text{ at } \lambda = 10.6\,\mu .$$

Laser bandwidths of $\sim$ 1 GH_z are presently available in CO_2 lasers at 10.6μ, and it is expected that much larger bandwidths will be available in the future. Neodymium-YAG lasers have bandwidths that could give time resolutions of $\sim$ 50 psec. A time resolution of 100 psec corresponds to a range resolution of 1.5 cm, and 1 psec to 0.015 cm. Optical radars are thus potentially capable of extremely high spatial resolution. In order to take advantage of this very high resolution, means for processing extremely fast optical transients must be developed. Most of the effort on this contract has been concerned with this problem. Although the bandwidth of the transmitted signal is necessarily very large if high resolution is desired, the actual information rate is not. The information desired from the received signal is an image of the target. If we assume that we want an image with 100 resolvable elements, each with a 10 bit gray scale and that we obtain the image in 1 millisecond, then the actual information rate is $\sim 10^6$ bits/sec. This is far less than the bandwidth of the transmitted waveform which could be 10^{12} Hz or higher. This observation leads to the conclusion that with proper signal processing, the desired image could be obtained with a relatively slow detection system.

A variety of waveforms could be used to obtain an image of the target. As mentioned above, the down range resolution is determined by the reciprocal of the bandwidth B of the signal and the cross range resolution by the total duration τ of the signal. The "average resolution" can be taken as

$$(\Delta x \Delta y)^{\frac{1}{2}} \sim (B\tau)^{\frac{1}{2}}$$

so that all signals with the same time-bandwidth product are equivalent as far as resolution. One possibility is to use a periodic train of short pulses that can be obtained conveniently from a mode-locked laser. This situation is illustrated in Figure 2a. The time between the pulses, if derived from a mode-locked laser, would typically be a few nanoseconds. The received signal will consist of a quasi-periodic train of longer duration pulses as shown in Figure 2b. Each of these pulses is a narrow band signal in times of the optical center frequency, and can be described in terms of an envelope $f(t)$ and an instantaneous phase $\phi(t)$. Adjacent received pulses

are nearly identical but there is a slow variation of f and ϕ that occurs over a time corresponding to the reciprocal of the doppler spread. The corresponding frequency domain description of the transmitted and received signals is shown in Figure 3.

One way of processing this signal is to range gate it and measure the amplitude and phase within each range element. Frequency analysis of the amplitude and phase within each range element gives the doppler spectrum within that range element. Measurements on each range element may then be used to construct the range-doppler image of the target. The signal could be processed by the scheme shown in Figure 4a. The signal is heterodyned against a local oscillator, detected, and range gated. If the local oscillator is at the same center frequency as the signal, a quadrature channel with the local oscillator shifted by $\lambda/4$ is also needed. If there is a frequency offset, this is not necessary. For a stationary target, the output of each range element will vary at the offset frequency and will be proportional to the signal received in that range element. If the target is rotating, the doppler spectrum from each range element will be superimposed on the signal. In this system, the detectors and the range gating electronics must be sufficiently fast to accommodate the desired time resolution of the received signal.

An alternate scheme is shown in Figure 4b. Here the signal is heterodyned against a mode-locked local oscillator which may be derived from a frequency shifted version of the transmitted signal. Heterodyning only occurs when the pulsed local oscillator is present so that the local oscillator provides the necessary range gating. Different optical propagation paths may be used to shift the position of the range gate as shown. This system does not require fast detectors. The time resolution is determined by the duration of the local oscillator pulse. The detectors need only respond to the if frequency.

An experiment was carried out to demonstrate this type of imaging. The experiment is shown schematically in Figure 5. The source used was a cw mode locked neodymium-YAG laser that emitted pulses of $\sim$ 100 psec. duration and with a separation of $\sim$ 3 nsec. The beam was expanded to a diameter of $\sim$ 6 cm. and illuminated the target. The polarized component of the return signal was reflected from the Glan-Thompson prism and was shifted in frequency by 40 MHz by an acoustic modulator. It was then heterodyned against a local oscillator derived from the transmitted beam as shown.

The target consisted of a bar holding two retroreflectors that were separated by a distance of 3.5 cm. The target was rotated at 0.5 rps about a horizontal axis. The sweep of the spectrum analyzer was initiated when the bar was at 45° with the upper half receding from the transmitter, and was completed before the target had rotated appreciably. The target was slowly scanned in range, and a spectrum was taken at corresponding points in each revolution. This slow scan in range allowed the various range elements of the signal to be measured sequentially and eliminated

the need for the parallel channels. The resulting signal was displayed on a storage scope. The horizontal position of the beam was scanned in synchronism with the spectrum analyzer sweep and the vertical position was scanned along with the target motion. The output of the spectrum analyzer modulated the beam intensity. This arrangement produced a range-doppler image directly. Such an image is shown in Figure 6. The upper portion shows the results with the laser operating on a single mode (no range resolution) and the lower portion shows the results with the laser mode-locked. The excellent spatial resolution ($\sim$ 2 cm) is evident.

Although this type of signal processing is capable of excellent time resolution, it is inefficient in the use of the received signal energy. Even for the case shown in Figure 4b, where parallel range samples are taken, much of the signal is wasted due to the fact that it must be split among the separate channels for each range element. This is a fundamental problem in any time sampling system. Efficient use of the signal would require some kind of a fast switch or beam deflector to switch the various range elements of the signal to different detectors or it would require a fast detector capable of resolving the time variation of the received signal. As has been mentioned above, the actual information rate of the signal is relatively low so there should exist techniques to process the signals that do not require wide bandwidths. One method is sampling in the frequency domain rather than in the time domain. This type of processing is discussed in detail in the next section. Its success arises from the fact that it is possible to spatially separate the frequency components of an optical signal with a passive device, a spectrometer. This will allow a measurement of the Fourier Transform of the optical signal in an efficient way. It is not possible to perform the same separation of the time segments of a signal without a fast, active element. The frequency domain sampling also offers the possibility of performing additional signal processing operations.

SECTION 2

FREQUENCY DOMAIN SAMPLING

2.1 Analysis

We will first consider the application of frequency domain sampling to the measurement of a repetitive train of extremely fast optical signals. The signal can be represented as a Fourier series

$$S(t) = \sum_{n=N}^{n=N} S_n \cos\left[(\omega_o + n\Omega)t + \varphi_n\right]$$

$$= \begin{cases} s(t)\cos\left(\omega_o t + \Phi(t)\right) & -T/2 \angle 0 \angle T/2 \\ \text{repeats every } T = \dfrac{2\pi}{\Omega} & \end{cases} \qquad 2.1$$

The quantities that are to be measured are $s(t)$, the instantaneous amplitude, and $\Phi(t)$, the phase of the signal. It will be assumed throughout that the signal is narrow band in terms of the optical center frequency ω_o, although it may be very wide band in terms of detector capabilities. The Fourier coefficients are given by

$$S_n \sin\varphi_n = -1/T \int_{-T/2}^{T/2} s(t)\sin\left(n\Omega t - \Phi(t)\right) dt$$

$$S_n \cos\varphi_n = +1/T \int_{-T/2}^{T/2} s(t)\cos\left(n\Omega t - \Phi(t)\right) dt \qquad 2.2$$

The general form of the signal processor is shown in Figure 7. The signal is first combined on a beam splitter with a reference waveform. This waveform will be denoted by

$$R(t) = \sum_{n=N}^{n=N} r_n \cos\left[(\omega_o + \omega_1 + n\Omega)t + \vartheta_n\right]$$

$$= \begin{cases} r(t)\cos\left[(\omega_o + \omega_1)t + \theta(t)\right] & -T/2 \angle 0 \angle T/2 \\ \text{repeats every } T = 2\pi/\Omega & \end{cases} \qquad 2.3$$

This reference waveform is periodic with the same period as the original signal, but its optical center frequency is shifted by an amount ω_1. It is assumed that $\omega_1 \ll \Omega \ll \omega_0$. The composite signal leaving the beam splitter is

$$C(t) = \sum_{n=-N}^{n=+N} \Big(S_n \cos\left[(\omega_0 + n\Omega)t + \varphi_n\right] + r_n \cos\left[(\omega_0 + \omega_1 + n\Omega)t + \vartheta_n\right]\Big) \qquad 2.4$$

The spectrum of this signal is shown schematically in Figure 7. This signal is then passed through a bank of narrow band optical filters. These filters are centered on the lines of the spectrum of C(t). (The lines are actually doublets as shown in Figure 7 , but the spacing of the doublet is small by assumption). The filters will all be assumed to be identical. The transmission of the m th filter for the n th spectral line will be denoted by $T_m(\omega_n)\, e^{i\psi(m,n)}$. Since the filters are identical, the transmission of a given line depends only on its displacement from the center frequency of the filter so that the transmission may be written

$$T(m-n)\, e^{i\psi(m-n)}$$

The output of the m th filter is given by

$$F_m = \sum_n T(m-n) \Big\{S_n \cos\left[(\omega_0 + n\Omega)t + \varphi_n + \psi(n-m)\right] + r_n \cos\left[(\omega_0 + \omega_1 + n\Omega)t + \vartheta_n + \psi(n-m)\right] \qquad 2.5$$

Each of these outputs is the square law detected to give a signal

$$\begin{aligned} G_m = \sum_n \sum_{n'} T(n-m)\, T(n'-m) &\Big\{S_n \cos\left[(\omega_0 + n\Omega)t + \varphi_n + \psi(n-m)\right] \\ &+ r_n \cos\left[(\omega_0 + \omega_1 + n\Omega)t + \vartheta_n + \psi(n-m)\right]\Big\} \cdot \\ &\Big\{S_{n'} \cos\left[(\omega_0 + n'\Omega)t + \varphi_{n'} + \psi(n'-m)\right] \\ &+ r_{n'} \cos\left[(\omega_0 + \omega_1 + n'\Omega)t + \vartheta_{n'} + \psi(n'-m)\right]\Big\} \end{aligned} \qquad 2.6$$

The detectors do not respond at the optical frequency so that only the difference terms in the products of cosines are significant. This gives

$$\bar{G}_m = \frac{1}{2} \sum_{n\,n'} T(n-m)\, T(n'-m) \Big\{ S_n S_{n'} \cos\left[(n-n')\Omega t + \varphi_n - \varphi_{n'} + \psi(n-m) - \psi(n-m)\right]$$

$$+ r_n r_{n'} \cos\left[(n-n')\Omega t + \vartheta_n - \vartheta_{n'} + \psi(n-m) - \psi(n'-m)\right]$$

$$+ S_n r_{n'} \cos\left[(n-n')\Omega t - \omega_1 t + \varphi_n - \vartheta_{n'} + \psi(n'-m) - \psi(n-m)\right] \qquad 2.7$$

$$+ S_{n'} r_n \cos\left[(n-n')\Omega t + \omega_1 t - \varphi_{n'} + \vartheta_{n'} + \psi(n-m) - \psi(n'-m)\right]$$

Each of these signals is now filtered with a narrowband electrical filter centered at ω_1. This eliminates all terms in the above expression except those for which $n' = n$. The resulting signal is

$$H_m = \sum_n T(n-m)^2 S_n r_n \cos(\omega_1 t - \varphi_n + \vartheta_n) \qquad 2.8$$

Here the phase factor of the optical filters has dropped out. Each of these outputs is now multiplied by $\cos(\omega_2 + m\Omega_2)t$ where ω_2 and Ω_2 are chosen at will (but with $\Omega_2 \ll \omega_2$). They are then summed to give

$$W(t) = \frac{1}{2} \sum_n \sum_m T(n-m)^2 S_n r_n \Big\{ \cos\left[(\omega_1 + \omega_2 + M\Omega_2)t - \varphi_n + \vartheta_n\right]$$

$$+ \cos\left[(\omega_2 - \omega_1 + M\Omega_2)t + \varphi_n - \vartheta_n\right]\Big\} \qquad 2.9$$

This may be written in a more convenient form by letting $p = n-m$ and eliminating m. The result is

$$W(t) = \frac{1}{2}\left(\sum_p T(p)^2 \cos p\Omega_2 t\right)\left(\sum_n S_n r_n \cos\left[(\omega_1 + \omega_2 + n\Omega_2)t - \varphi_n + \vartheta_n\right]\right)$$

$$+ \frac{1}{2}\left(\sum_p T^2(p)^2 \sin p\Omega_2 t\right)\left(\sum_n S_n r_n \sin\left[(\omega_1 + \omega_2 + n\Omega_2)t - \varphi_n + \vartheta_n\right]\right)$$

$$+ \frac{1}{2}\left(\sum T^2(p)^2 \cos p\Omega_2 t\right)\left(\sum_n S_n r_n \cos\left[(\omega_2 - \omega_1 + n\Omega_2)t + \varphi_n - \vartheta_n\right]\right)$$

$$+ \frac{1}{2}\left(\sum T(p)^2 \sin p\Omega_2 t\right)\left(\sum S_n r_n \sin\left[(\omega_2 - \omega_1 + n\Omega_2)t + \varphi_n - \vartheta_n\right]\right)$$

We now consider some special cases. If the filters are sufficiently narrow that they only pass one spectral line, then $T(p) = \delta(p)$ and

$$W(t) = \frac{1}{2}\ \Sigma s_n r_n \cos\left[(\omega_1 + \omega_2 + n\Omega_2)\,t - \varphi_n + \vartheta_n\right]$$
$$+ \frac{1}{2}\ \Sigma s_n r_n \cos\left[(\omega_1 + \omega_2 + n\Omega_2)\,t + \varphi_n - \vartheta_n\right] \qquad 2.11$$

Suppose now that the reference waveform consists of a train of extremely short pulses. In this case r_n is essentially constant and $\vartheta_n = 0$. We have then

$$W(t) \sim \frac{1}{2}\ \Sigma s_n \cos\left[(\omega_1 + \omega_2 + n\Omega_2)\,t - \varphi_n\right]$$
$$+ \frac{1}{2}\ \Sigma s_n \cos\left[(\omega_1 - \omega_2 + n\Omega_2)\,t + \varphi_n\right] \qquad 2.12$$

Reference to Eq. 2.1 will show that

$$W(t) = \frac{1}{2}\ S(-\alpha t) \cos\left[(\omega_1 + \omega_2)\,t - \Phi\,(-\alpha\,t)\right]$$
$$+ \frac{1}{2}\ S(\alpha\,t) \cos\left[(\omega_1 - \omega_2)\,t + \Phi\,(\alpha t)\right] \qquad 2.13$$
$$= W_+\,(t) + W_-\,(t)$$

for $-T_2/2 \angle 0 \angle T_1/2$

repeating with period $T_2 = 2\Pi/\Omega_2$

and with $\alpha = \dfrac{\Omega_2}{\Omega}$

The second term is this an exact replica of the original optical signal but with a time scale that has been stretched by a factor Ω/Ω_2. The center frequency of the signal has also been changed from the optical frequency ω_o to an r.f. frequency $\omega_1 - \omega_2$. The first term is a time reversed version of the optical signal, stretched in time, and with a center frequency $\omega_1 + \omega_2$. The signal processor has extracted the amplitude and phase of each of the componets of the line spectrum of the original optical signal and has imposed them on a line spectrum at an r.f. frequency. This synthesizes the original signal. The signal and its time reversed version may be readily separated by the proper choice of ω_1 and ω_2 together with frequency filtering.

Let us now consider the more general case where r_n and ϑ_n are arbitrary. The component at $\omega_2 - \omega_1$ is

$$W(t) = \frac{1}{2}\ \Sigma s_n r_n \cos\left[(\omega_1 - \omega_2 + n\Omega_2)\,t + \varphi_n - \vartheta_n\right] \qquad 2.14$$

The cross correlation of the signals s(t) and r(t) is

$$\int_{-T/2}^{T/2} S(t)R(t-\tau)dt = \frac{T}{2}\sum_n S_n r_n \cos\left[(\omega_o + n\Omega)\tau + \varphi_n - \vartheta_n\right] \qquad 2.15$$

The function $W_-(t)$ may be seen to be a repetitive time display of the cross correlation function. The function $W_+(t)$ is just a time reversed version of this signal. In the case where S(t) and R(t) are identical, the processor gives the autocorrelation function as a function of time; i.e., it behaves as a matched filter. In the case where R(t) is a train of pulses of finite duration pulses rather than extremely narrow pulses, the original signal is received with a degraded time resolution given by the duration of the pulses constituting R(t).

We may now return to the more general case given in Eq. 2.10. Let

$$\begin{aligned} \sum_p T(p)^2 \cos p\Omega_2 t &= T_c(t) \\ \sum T(p)^2 \sin p\Omega_2 t &= T_s(t) \end{aligned} \qquad 2.16$$

We note that if the bandpass of the optical filters are symmetric; i.e., if $|T(p)| = |T(-p)|$, then $T_s(t) = 0$.

$$\begin{aligned} G(t) &= \sum s_n r_n \cos\left[(\omega_1 + \omega_2 + n\Omega_2)t - \varphi_n + \vartheta_n\right] \\ &= g(t)\cos\left[(\omega_1 + \omega_2)t + \gamma(t)\right] \qquad 2.17 \end{aligned}$$

$$(\text{periodic at } T_2 = 2\pi/\Omega_2)$$

For a narrowband waveform, it will be true that

$$\sum S_n r_n \sin\left[(\omega_1 + \omega_2 + n\Omega)t - \varphi_n + \vartheta_n\right] = g(t)\sin\left[(\omega_1 + \omega_2)t + \gamma(t)\right] \qquad 2.18$$

So that we have for the $\omega_1 + \omega_2$ component of Eq. 2.10

$$W_+ = T_c(t)\,g(t)\cos\left[(\omega_1 + \omega_2)t + \gamma(t)\right] + T_c(t)g(t)\sin\left[(\omega_1 + \omega_2)t + \gamma(t)\right] \qquad 2.19$$

A similar expression holds for W_-. The shape of the filter transmission function multiplies the output of the system by a known function of time. The result that would be obtained with very narrow filters can be computed from the result obtained from wider filters. Alternately, the filter functions could be chosen to perform additional signal processing operations.

The entire discussion above has been concerned with repetitive signals. The frequency domain sampling technique is not restricted to this case. It may be applied to the measurement of a single optical transient. The processing is somewhat more complicated in this case because it corresponds to heterodyning with zero difference frequency and care must be taken to avoid spectral overlapping. A system to perform this measurement is illustrated schematically in Figure 9. We assume again a signal and a reference

$$S(t) = \frac{1}{(2\pi)^{\frac{1}{2}}} \int e^{+i\omega t}\, s(\omega) d\omega$$

$$R(t) = \frac{1}{(2\pi)^{\frac{1}{2}}} \int e^{i\omega t}\, r(\omega)\, d\omega$$

The signals are combined on a beamsplitter to produce a composite spectrum

$$c(\omega) = s(\omega) \pm r(\omega)$$

The two signs are obtained from opposite sides of the beamsplitter. The composite signal is then passed through a filter bank. At the output of each filter a signal

$$F_m(\omega) = R\left(S(\omega) \pm r(\omega)\right) T_m(\omega)$$

is obtained. This is square law detected and integrated over time to obtain

$$G_m = \int_{-\infty}^{\infty} |s(\omega) \pm r(\omega)|^2\, |T_m(\omega)|^2\, d\omega$$

$$= \int_{-\infty}^{\infty} \left\{ |s(\omega)|^2 \pm \mathrm{Re}\left(r(\omega)s^*(\omega)\right) + |r(\omega)|^2 \right\} T_n(\omega)\, d\omega$$

The difference between the plus and minus signals is then taken to give

$$U_n = 2 \int_{-\infty}^{\infty} \mathrm{Re}\left(r(\omega)s^*(\omega)\right) T_m(\omega)\, d\omega$$

If the filters are extremely narrow, $T_n(\omega) \approx \delta(\omega-\omega_m)$ and

$$U_m = 2 \,\mathrm{Re}\left(r(\omega_m)\, s^*(\omega_m)\right)$$

If the same operation is repeated with the reference wave shifted by $\lambda/4$, the output

$$U_m' = 2 \,\mathrm{Im}\left(r(\omega_m)\, s^*(\omega_m)\right)$$

will be obtained. We thus obtain a sampled version of $r(\omega)\, S^*(\omega)$. This quantity is the Fourier Transform of the cross correlation function; i.e.

$$\int_{-\infty}^{\infty} R(t)\, S\,(t-\tau)\, dt = \int_{-\infty}^{\infty} e^{i\omega t}\, r(\omega)\, s^*(\omega)\, d\omega$$

These parallel outputs may be used to reconstruct the signal at any desired frequency and repetition rate in a manner identical to the previous discussion.

2.2 Discussion and Experimental Implementation

The analysis of the previous section described the operation of the frequency sampler in the time domain. Figure 8 shows the situation in the frequency domain, and illustrates why the turn frequency domain sampling has been used. The various components of the line spectra of $R(t)$ pass through the filters, are isolated, and are distributed to separate detectors. If an appropriate local oscillator were available at each detector, the amplitude and phase of each of the components could be measured. This would completely characterize the signal. Just such a set of local oscillators can be obtained by filtering a periodic train of short pulses through the same filter bank as the signal. Each channel can be operated in the quantum noise limited regime, and all of the energy received in each channel is used.

An alternate way of looking at the operation of the system is to consider the response of one of the narrow band filters to a short optical pulse. The output of the filter has a duration corresponding to the reciprocal of the bandwidth of the filter. This should be made comparable to the duration of the signal that is to be measured. The reference signal can thus heterodyne with the signal over its entire duration. The precise details of the resulting signal are given above.

We may now consider means of implementing such a detection system. One of the first considerations is the resolving power required of the filters. Let us assume that the line shape of the filter is

$$T_{(p)} = \frac{\sin \alpha p}{\alpha p}$$

where the first zeros occur at $\alpha p = \pm \Pi$. The modulating functions are

$$T_s(t) = 0$$

$$T_c(t) = \sum_{p=-P}^{p=P} \frac{\sin^2 \alpha p}{(\alpha\, p)^2} \cos p\,\Omega_2 t$$

This is a periodic function with period $T_2 = 2\pi / \Omega_2$. We may rewrite this in the form

$$T_c(t) = \underline{1} + \frac{2}{\alpha^2} \sum_{p=1}^{p=P} \frac{\sin^2 \alpha p}{p^2} \cos p\,\Omega_2 t$$

For values of $\alpha < \pi$ this simply represents a triangular pulse extending from $-\alpha/\Omega < t < \alpha/\Omega$ as shown in Figure 10. When $\alpha = \pi$ the pulse extends over the entire interval $-T/2 < t < T_2/2$. For larger values of α, the base line lifts as shown in the figure. For the particular values $\alpha = RN$, the function $T_c(t) = 1$. The reason for this is shown in Figure 10. Although the filter has finite transmission off its center frequency, its transmission for the lines of the spectrum of $S(t)$ is zero except for the line on center.

For ease in data interpretation, the filters should be made quite narrow (or they should satisfy the condition illustrated in Figure 11). They should not, however, be made so narrow that they are capable of resolving the if frequency, since this will pervent the heterodyning of the signal and the reference waveforms. The bandwidth $\Delta\omega$ of the filters should be in the range $\omega_{if} < \Delta\omega < \Omega$. For a typical mode locked laser, $\Omega/2\pi \sim 3 \times 10^8$ Hz, at a wavelength of 1.06 μ, $\omega_o/2\pi = 3 \times 10^{14}$ Hz. This corresponds to a resolving power of $\omega_o/\Delta\omega \sim 10^6$. This resolving power is easily obtainable with a Fabey-Perot etalon. It can be obtained with more difficulty with a grating, a large grating, possibly with several passes would be required. The grating approach, however, has several advantages which will be discussed later.

The number of filters required is determined by the desired time resolution (which is ultimately determined by the bandwidth of the reference signal). Figure 12 shows the response of the system to an amplitude step for a filter bank employing 5, 11 and 21 filters. Figure 13 shows the amplitude and phase of the response of the system to a pulse of constant amplitude and linearly increasing phase (a frequency offset) for a filter bank with 11 components, and Figure 14 for one with 21 components. Figure 15 shows the response to a chirped pulse for 11 and 21 components. These responses were computed by calculating the Fourier coefficients of the applied waveform, truncating them at the desired number of components and then reconstructing the series with the truncated set of coefficients.

The problems involved in the experimental demonstration of the frequency domain sampling technique are:

1. attainment of sufficient resolving power in the optical filter bank
2. simultaneous detection of the signals from each of the filters
3. modulation of the output of each detector by the appropriate modulation waveform
4. recombination of the modulated outputs to regenerate the time-scaled version of the original signal.

The first of these requirements determines the type of spectrometer that is required. The spectrometer must have:

1. a resolving power of the order of 10^6
2. high throughput
3. produce an output of all the frequency components of the incident beam simultaneously.

A Fabry Perot etalon can satisfy the first two of these requirements readily. It does not, however, satisfy the third. When a Fabry Perot etalon is operated with a collimated input beam, it acts as an optical band pass; i.e., it passes the wavelength to which it tuned, with high transmission, and it reflects all the other wavelengths with low loss. If it is operated with an input beam from an extended source or one with more divergence than the diffraction limit of its aperture, then it acts as a spectrometer and produces the characteristic circular fringe pattern. This, however, entails a loss of signal power. A plane Fabry Perot basically provides a transmission that depends on the angle of propagation of the beam with respect to the normal to the reflectors. It has a high throughput for components at the proper frequency and angle. The best that can be done is to arrange the divergence of the input beam so that only one free spectral range is illuminated. The total power transmitted in a given ring is then given by the total power incident at the frequency corresponding to the ring divided by the finesse of the interferometer.

The ease with which a high resolving power can be obtained with a Fabry Perot etalon makes it attractive, however, and it will be used for a demonstration of the frequency domain sampling technique.

The most convenient form of spectrometer for use in the system is a grating. Grating can have a high throughput and produce a spatially disfused output at all frequencies simultaneously. The main problem is that of obtaining sufficient resolution. Conventional gratings are limited to a resolution of the order of 500,000. Echelle gratings are capable of resolutions in the range of 500,000 to 2,000,000. For any type of multiple beam dispersive device, the resolution will be determined by the difference in transit time between the shortest and the longest path in the device; i.e.,

$$\Delta f \sim \frac{1}{\Delta \tau}$$

and

$$R = \frac{f}{\Delta f} = f \, \Delta \tau$$

For a grating used in a Littrow arrangement as shown in Figure 16,

$$\Delta\tau = \frac{2\ W \sin\alpha}{c}$$

and

$$R = \frac{2\ W}{\lambda} \sin\alpha$$

Echelle gratings are typically operated with a diffraction angle $\alpha \sim 65^{o}$ so that $\sin\alpha \approx 0.9$. Thus to achieve a resolution of 10^6 at a wavelength of 1 micron, a grating of width

$$W = \frac{\tau\ R}{2 \sin\alpha} = 55 \text{ cm}$$

is required. This is an impractically large size for a single grating. The required resolution may be obtained by multiple diffractions. Two-pass and four-pass instruments have been fabricated and operated successfully. For a four-pass instrument the grating width is reduced to 14 cm, a size that is commerically obtainable at reasonable cost.

The required resolution for the frequency domain sampling system is obtainable easily with a Fabry Perot filter and with more difficulty with an echelle grating. We must now turn to the problem of performing the required signal processing after the dispersion is obtained. One means of performing this would be to implement the system exactly as shown in Figure 7. The output of the grating could be imaged upon a close packed array of detectors, one for each resoluable frequency element. The output of each detector could then be modulated in an electronic mixer with the appropriate modulation frequency and the results summed electronically to yield the desired output. There is no fundamental objection to this approach except for the difficulty involved in maintaining balance among all the separate channels and the large number of separate electronic channels that are needed.

Fortunately, the entire signal processing operation after dispersion can be conveniently and simply accomplished by a parallel optical processor. One form of this processor, which has been successfully demonstrated, is the frequency multiplexed Fabry Perot Interferometer (Ref. 1). This device simultaneously performs the detection, modulation and signal recombination required in the present case. The use of a Fabry Perot interferometer necessarily entails a loss of singal as discussed above, but the scheme may be extended to an echelle grating and this problem can be eliminated.

The form of the Fabry Perot multiplexer is illustrated schematically in Figure 17a. This figure illustrates the fringe pattern that would be observed if the etalon were illuminated by a line spectrum (in this case only four lines are shown). Figure 17b shows one full free spectral range. To use this output in the sampling system as originally described, one would have to direct each of these rings to a separate detector whose output is subsequently modulated. Schemes to do this involving axicom or sets of annular mirrors have been reported in Refs. 2, 3, but they become unweildy for a large number of channels. The entire problem can be solved by modulating the rings prior to detection. This can be accomplished by the so-called multizone disk (Ref. 1). The disk is shown schematically in Figure 18. It consists of a transparent substrate that is divided into a number of annular zones. The mean radius of each zone is centered on the rings that are observed in the focal plane of a Fabry Perot filter that is illuminated by the line spectrum. Each zone is divided into an equal number of transparent and opaque area, and the number of areas increase as the radius of the zone increases. Two such disks are placed in the plane of the Fabry Perot fringes, and one is rotated with respect to the other. Each line of the spectrum is thus chopped at a different frequency determined by the number of "teeth" in the zone and the rotational rate. The entire signal that is transmitted through the device is focussed onto a single detector. This performs an operation on the signal that is very nearly the one required to reconstruct the signal. Referring to Eq. 2.5, we see that the amplitude of each component is multiplied by a function sqr $(\omega_2 t + m\Omega_2 t)$ where sqr (ωt) is a square wave function that oscillates between 0 and 1, and has the same sign and zero crossings as cos (ωt). The derivation leading to Eq. 2.9 follows through exactly as before, except that the modulating functions are square waves rather than sin waves. If we arrange the disk so that the lowest modulating frequency is greater than 1/2 of the highest modulating frequency, then the higher harmonics of the square waves can be filtered out electrically and the desired output will be obtained.

The number of filter elements that can be obtained by this technique is limited only by the finesse of the interferometer. The maximum modulation frequency is determined by the number of elements that can be placed on the disk and by the rotation rate. The disk can be made by drawing it on a large scale with a computer controlled plotter and then reducing it photographically. It is reasonable to assume that the widths of the teeth in the zones can be made as small as 20-30 microns. For an inner zone of 1 cm diameter, this would give approximately 1000 elements. If the disk is rotated at 400 rps, a modulation frequency of 400 KHz can be obtained. The number of teeth in the outermost zone should be less than twice the number in the inner zone. This gives a total range of 400 KHz. If there are 40 zones on the disk, the frequencies can be spaced by 10 KHz. The repetition period of the reconstructed optical signal could be 100 microseconds in this case. The center frequency would be the i.f. frequency plus or minus the mean modulation frequency.

During the next period of this contract, an experimental demonstration of the frequency domain sampling using the multiplexed Fabry Perot interferometer will be carried out.

A preliminary experiment to demonstrate the feasibility of individually heterodyning the line components of the signal and the reference waves has been carried out. The experimental arrangement was similar to that shown in Figure 5. A scanning Fabry Perot filter was placed in front of the detector so that the lines of the spectrum of the combined signal and reference could be examined individually. The detected signal at the i.f. frequency (40 MHz) was rectified and displayed on an oscilloscope. The horizontal axis of the oscilloscope was scanned in synchronism with the spectrum analyzer. The resulting display is shown in Figure 19a. The target in this case was a plane mirror. The display shows the heterodyne signals from each of the lines of the combined signal and reference waveforms. In this figure, a little more than two free spectral ranges are shown. The oscillating bandwidth of the laser was somewhat greater than the free spectral range of the Fabry Perot (86 Hz) so that there is some overlapping of orders. When an additional mirror (~ 65% R) was placed in front of the target mirror, the display shown in Figure 19b was obtained. The two mirrors constitute a Fabry Perot filter. When operated in reflection, the filter exhibits minima at frequencies determined by $\Delta f = c/2\ell$. These minima may be seen in the figure. The location of the minima varied with the spacing of the mirrors as would be expected from the formula. The feasibility of heterodyning the components of the line spectrum individually was thus confirmed.

The multiplexing scheme used with the Fabry Perot can be applied to other types of dispersion elements such as an echelle grating. A possible arrangement is shown in Figure 20. The output of the grating is focussed in the direction normal to the dispersion by a cylindrical line. This line is then scanned by a beam deflector across a mesh whose transparency is shown schematically in the figure. The signal transmitted through the mask is then focussed into a detector. In addition to eliminating the inefficiency associated with the Fabry Perot, this scheme is capable of modulating at much higher frequencies. The modulation frequency is limited only by the speed of the beam deflector which may be mechanical, electrooptical or acousto-optical.

REFERENCES

1. J. G. Hirschberg, W. I. Fried, L. Hazelton, Jr., and A. Wouters, App. Opt. 8, p. 1979 (1971).

2. J. Katzenstein, App. Opt. 4, p. 263 (1965).

3. J. G. Hirschberg, and P. Plate, App. Opt. 4, p. 1375 (1965).

RANGE–DOPPLER IMAGING

a)

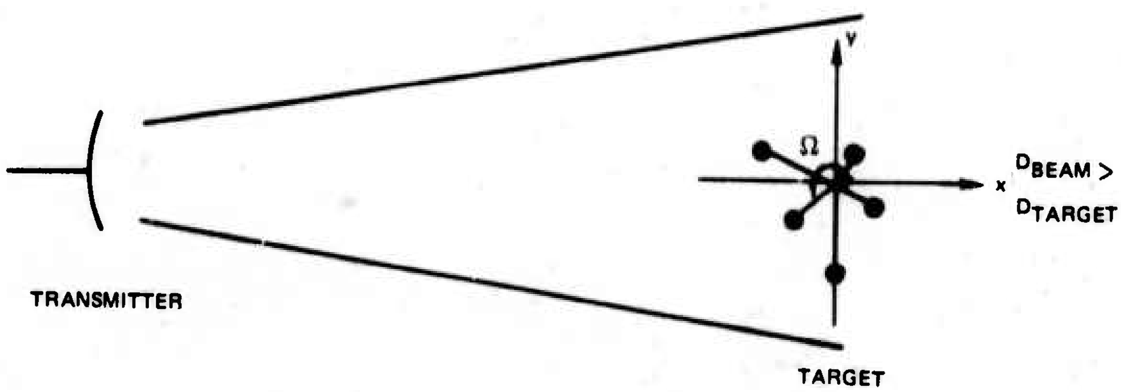

b) RANGE–DOPPLER IMAGE

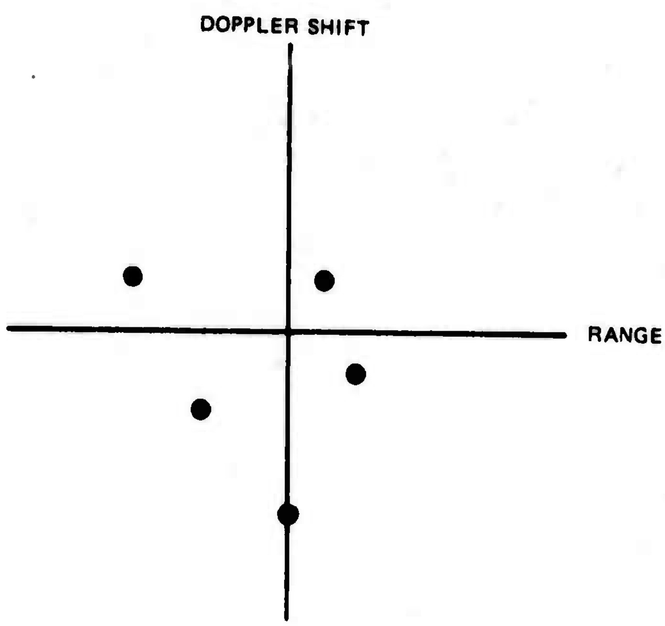

TIME DOMAIN DESCRIPTION

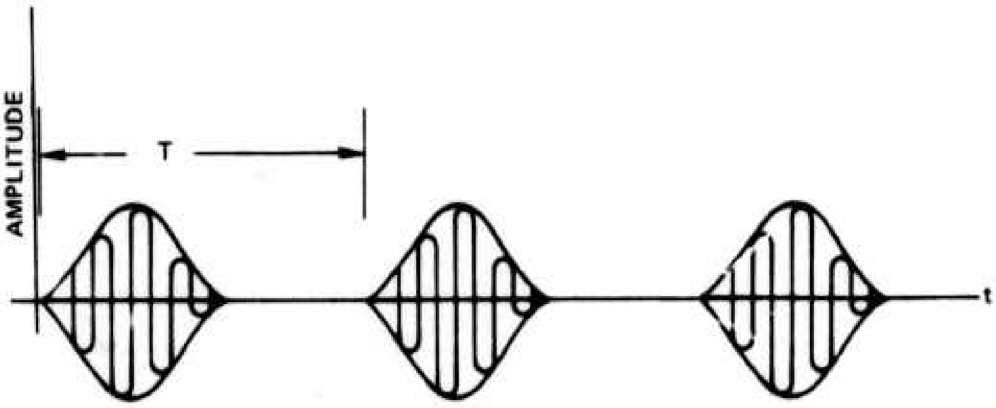

TRANSMITTED SIGNAL

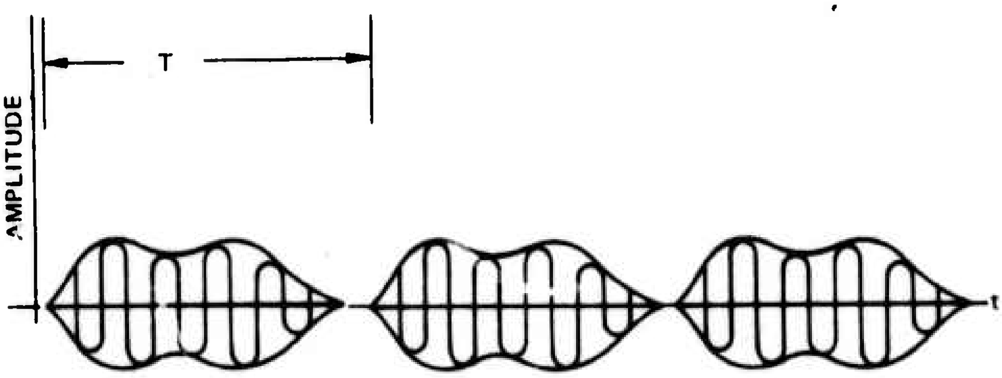

RECEIVED SIGNAL

$f(t) \cos (w_0 t + \Phi(t)$, REPEATS EVERY T

$f(t)$ AND $\Phi(t)$ HAVE A LONG TERM TIME VARIATION DUE TO THE DOPPLER SHIFT

M920479–42

FIG. 3

FREQUENCY DOMAIN DESCRIPTION

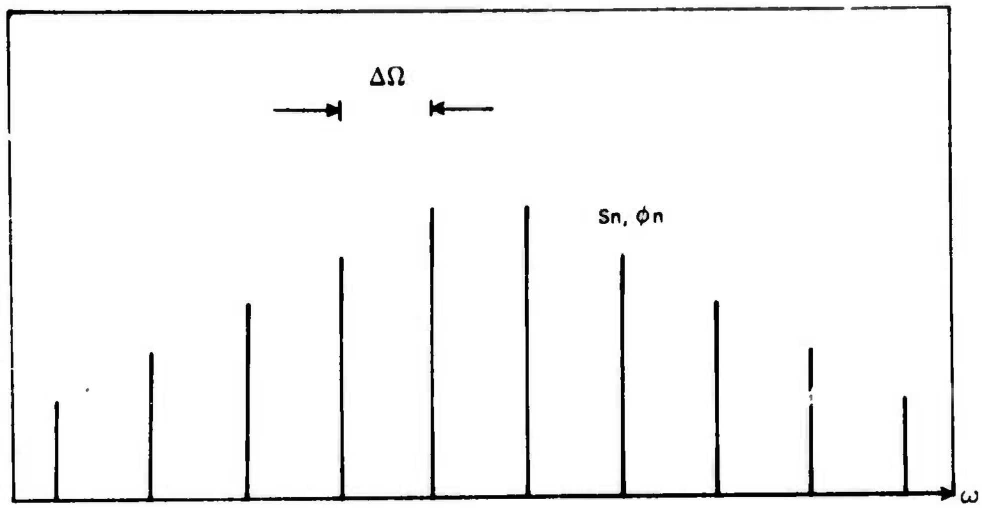

SPECTRUM OF TRANSMITTED SIGNAL

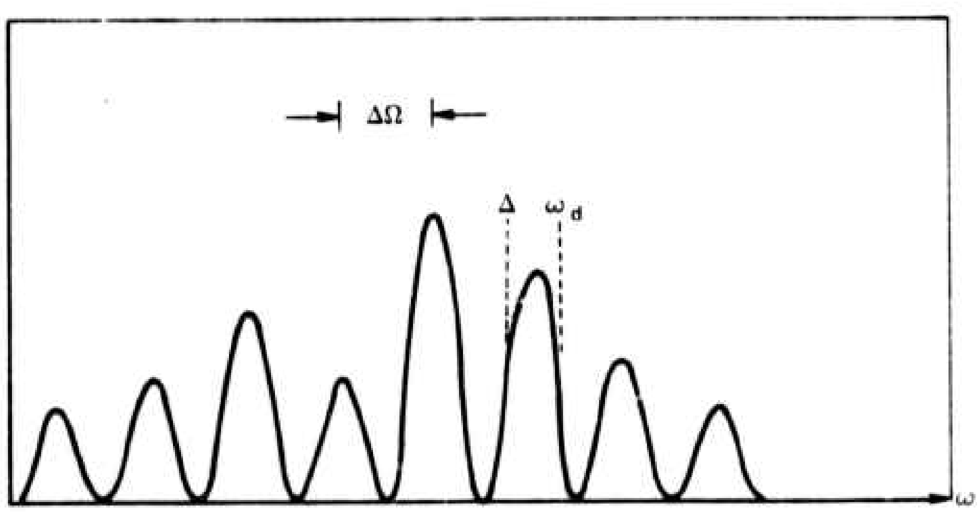

SPECTRUM OF RECEIVED SIGNAL

FIG. 4

RANGE GATING

a) ELECTRONIC

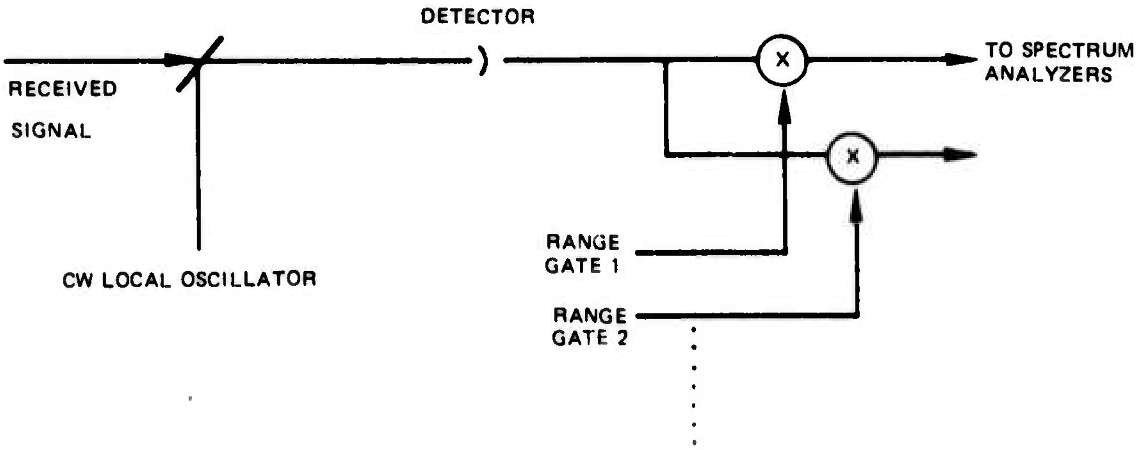

b) OPTICAL

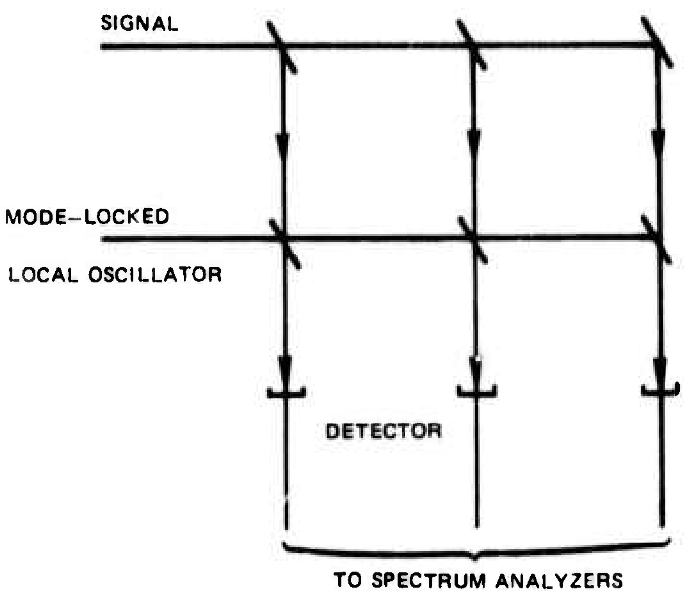

EXPERIMENTAL RANGE – DOPPLER SYSTEM

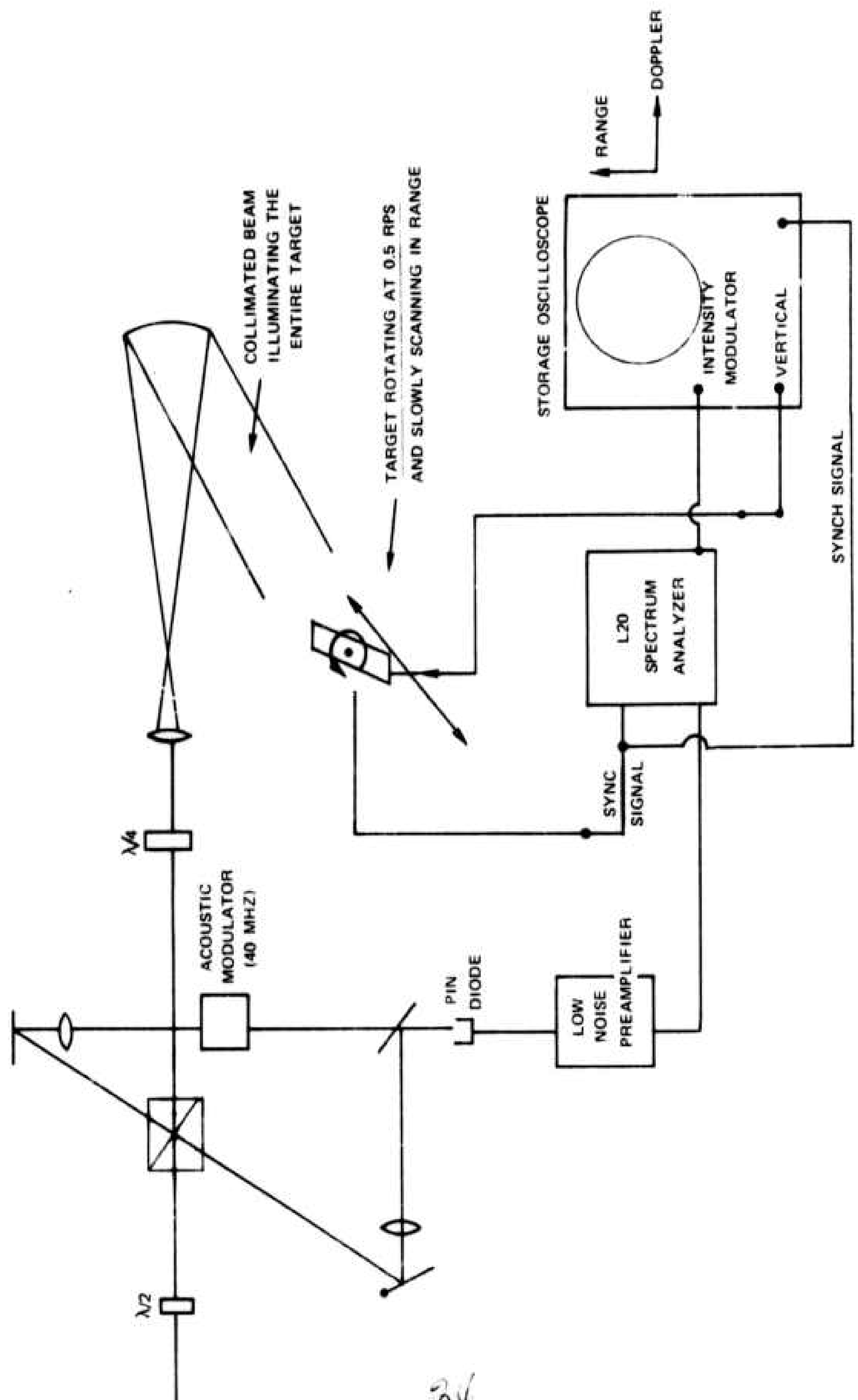

M920479-42

FIG. 6

RANGE–DOPPLER IMAGE OF A LABORATORY TARGET

1 DIV = 2.4 CM

RANGE

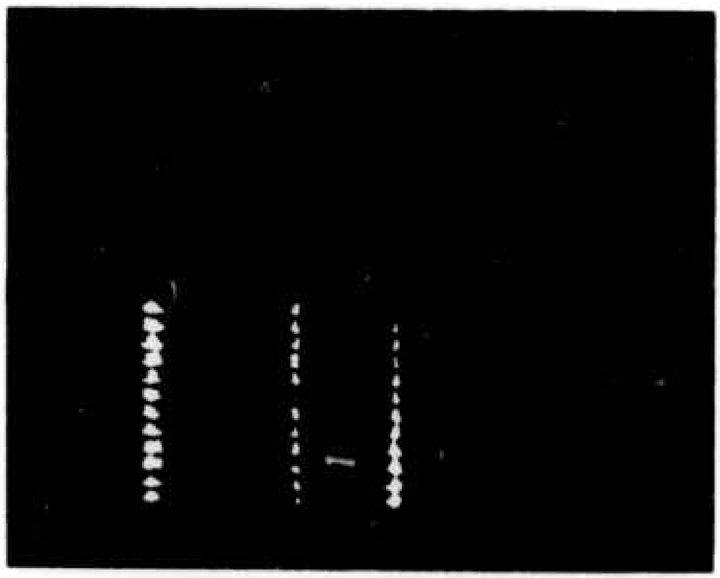

SINGLE MODE LASER

TARGET AXIS
DOPPLER
50 KC/DIV

RANGE

LASER MODE–LOCKED

TARGET AXIS
DOPPLER

M920479–24 FIG. 7

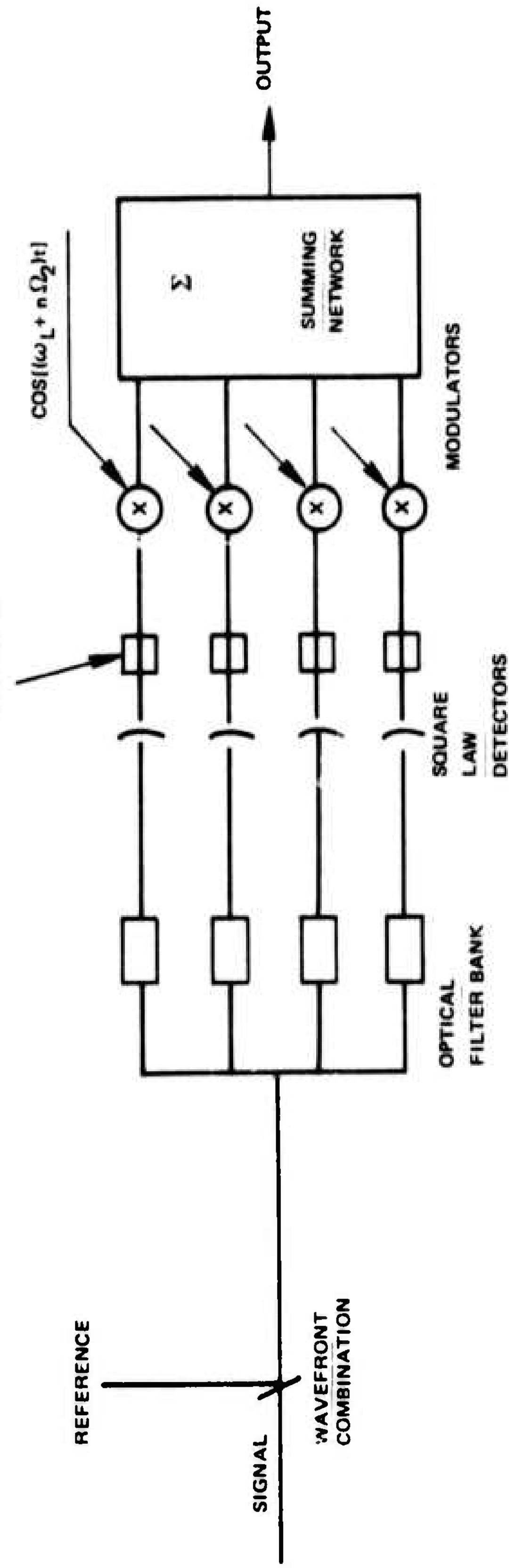

GENERAL FORM OF SIGNAL PROCESSOR

SPECTRA OF SIGNAL AND REFERENCE

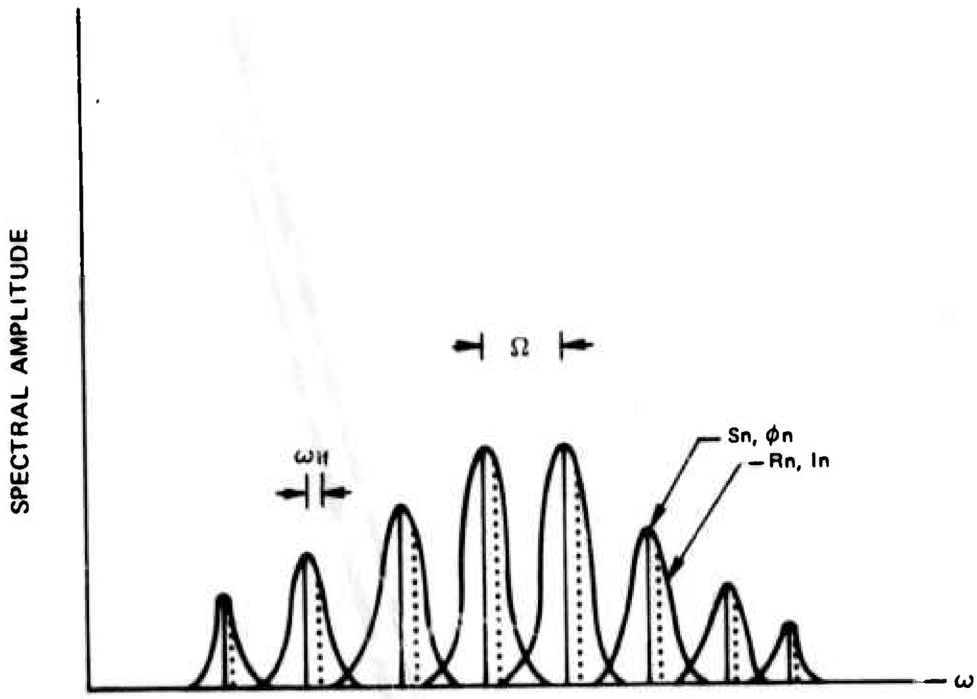

TRANSMISSION OF OPTICAL FILTERS

M920479–42

FIG. 9

FREQUENCY SAMPLING FOR A SINGLE OPTICAL TRANSIENT

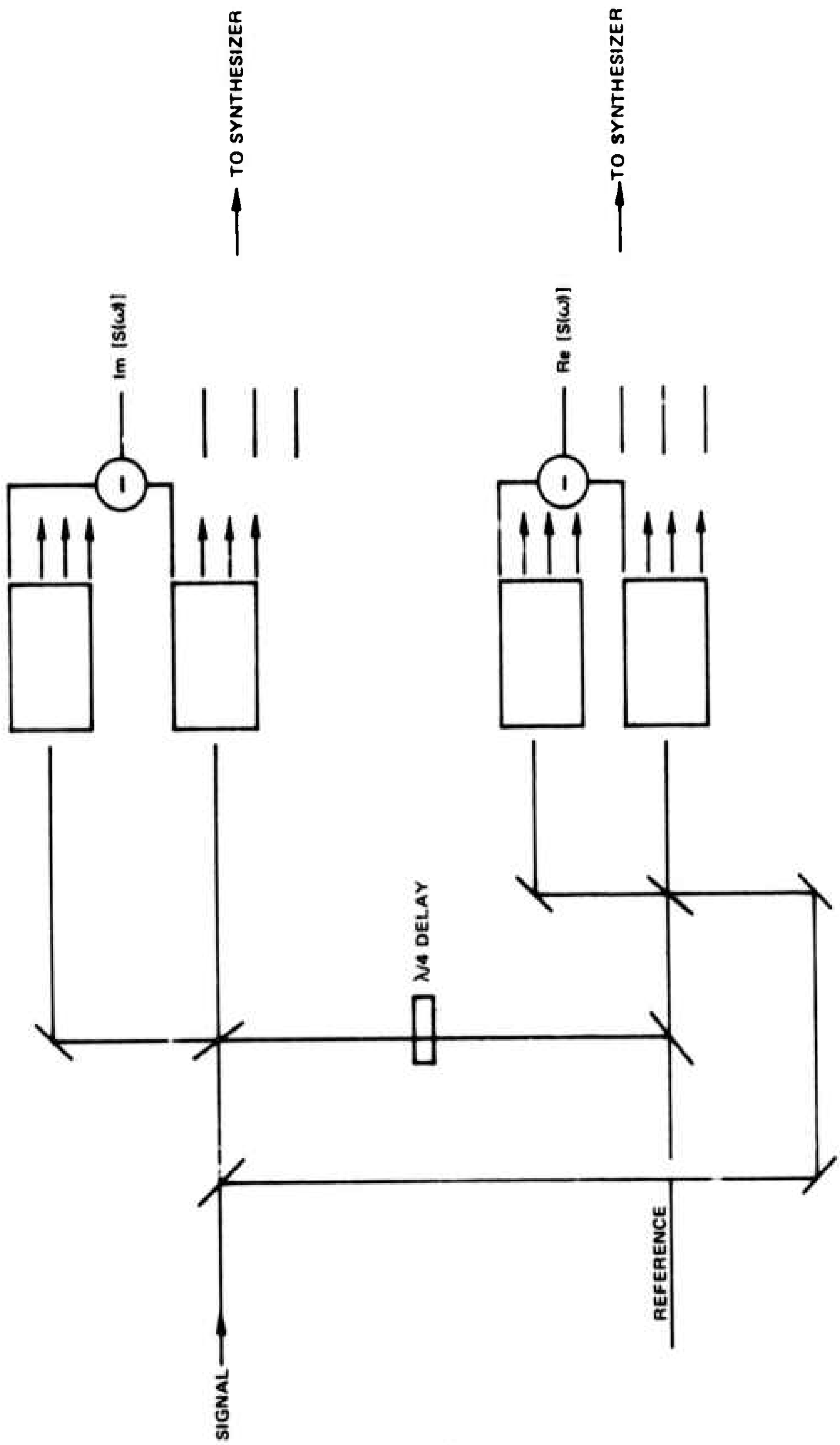

M920479–42

FIG. 10

BEHAVIOR OF T_c (t)

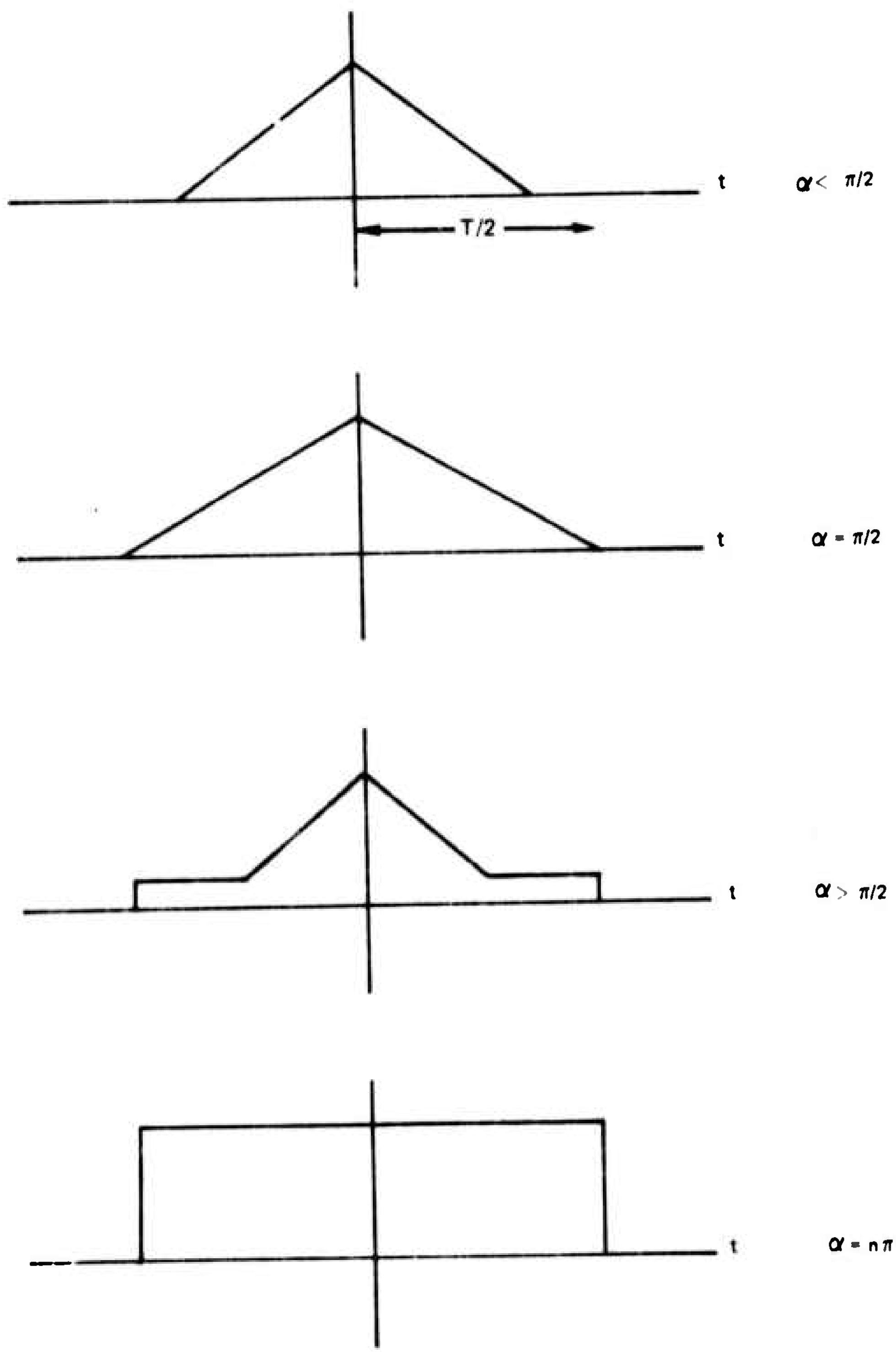

FIG. 11

TRANSMISSION OF LINE SPECTRUM THROUGH FILTER

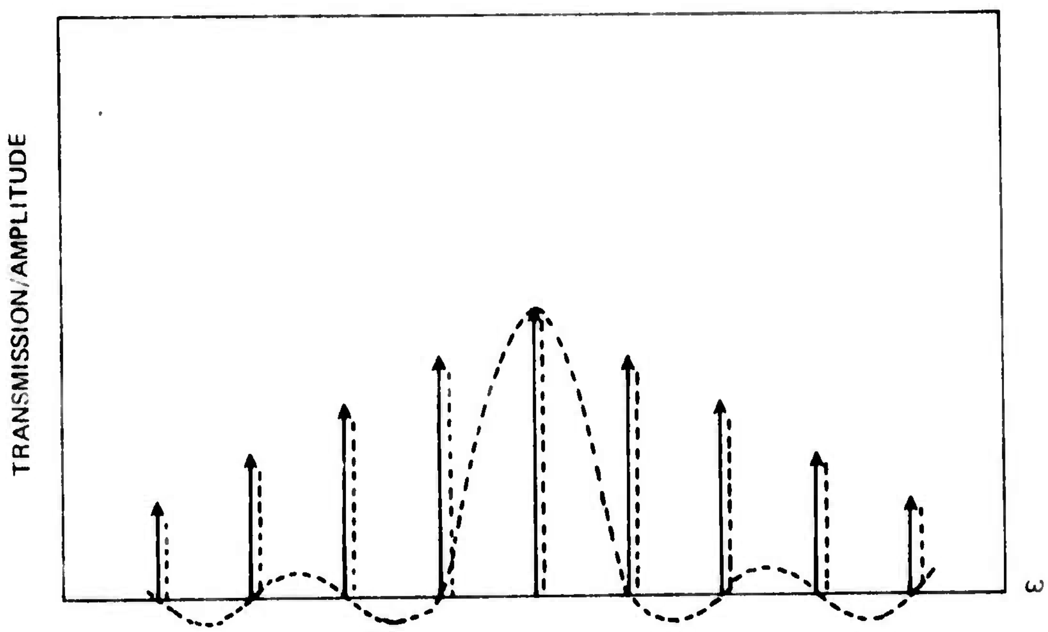

RECONSTRUCTION OF AMPLITUDE STEP

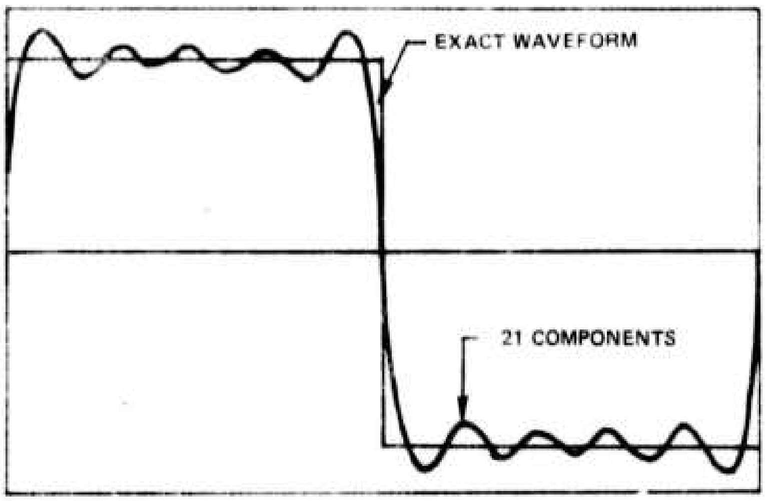

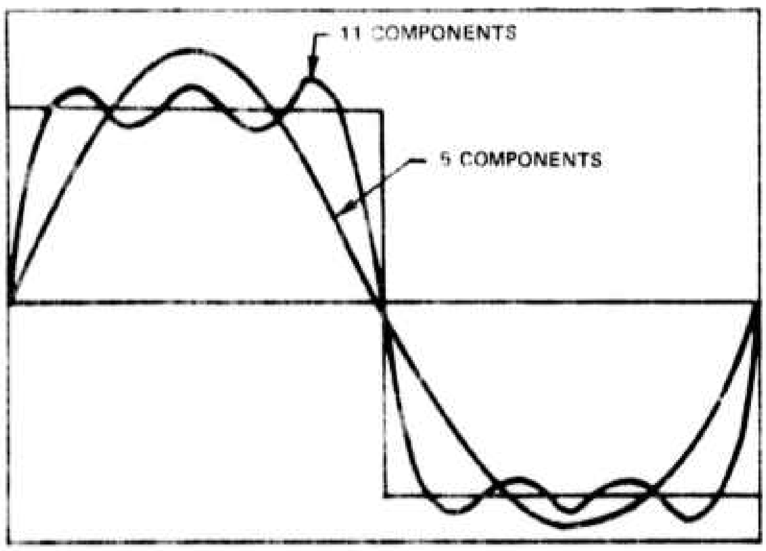

RESPONSE TO FREQUENCY STEP

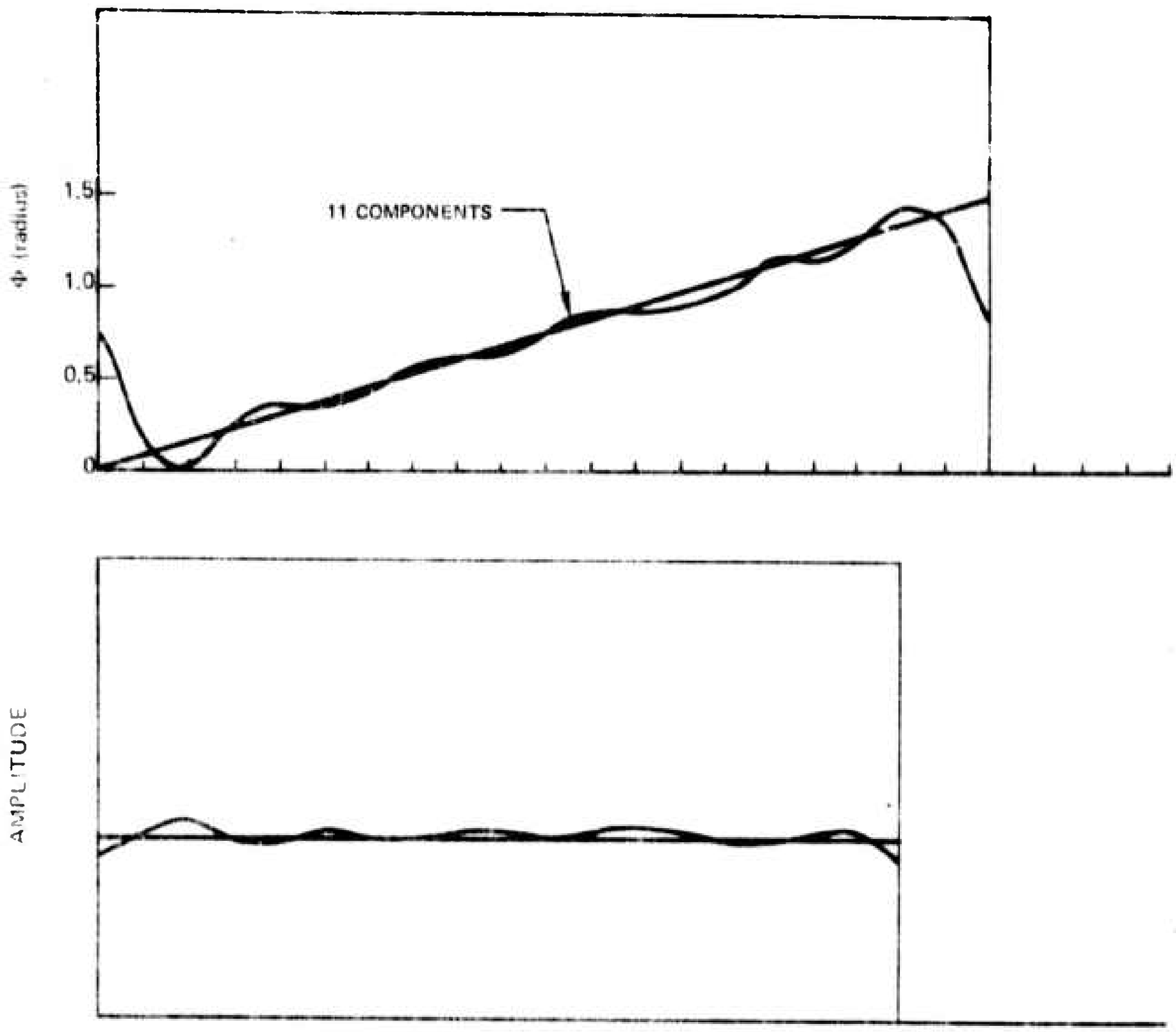

RESPONSE TO FREQUENCY STEP

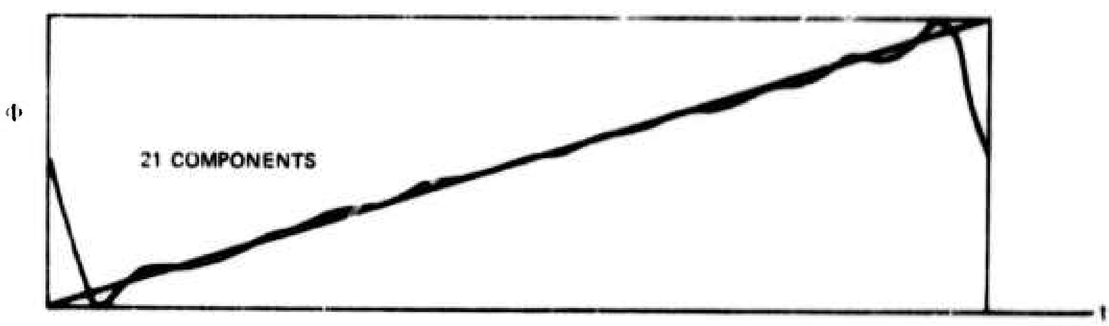

M920479–42

FIG. 15

RESPONSE TO CHIRPED PULSE

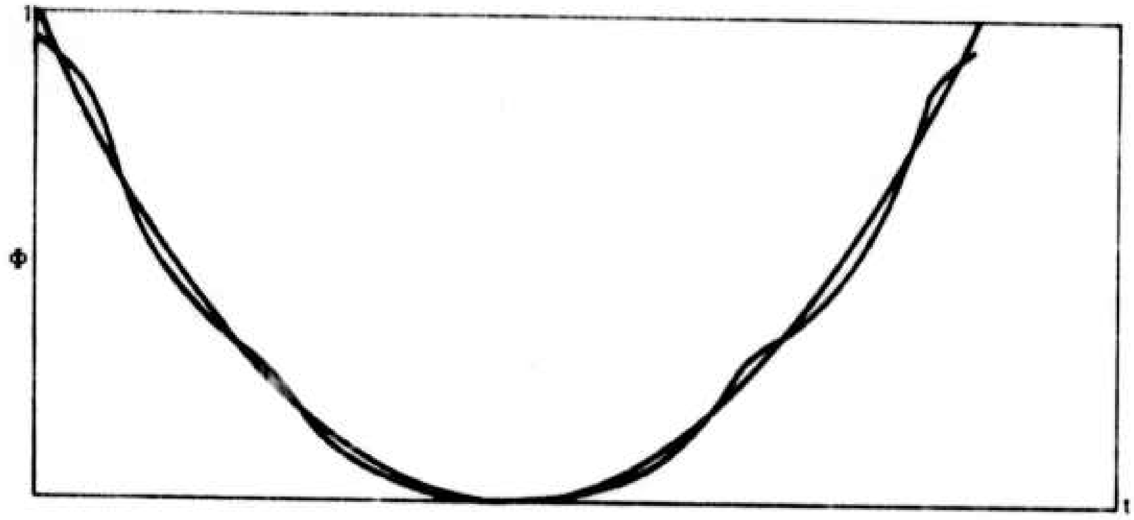

RESOLUTION OF ECHELLE GRATING

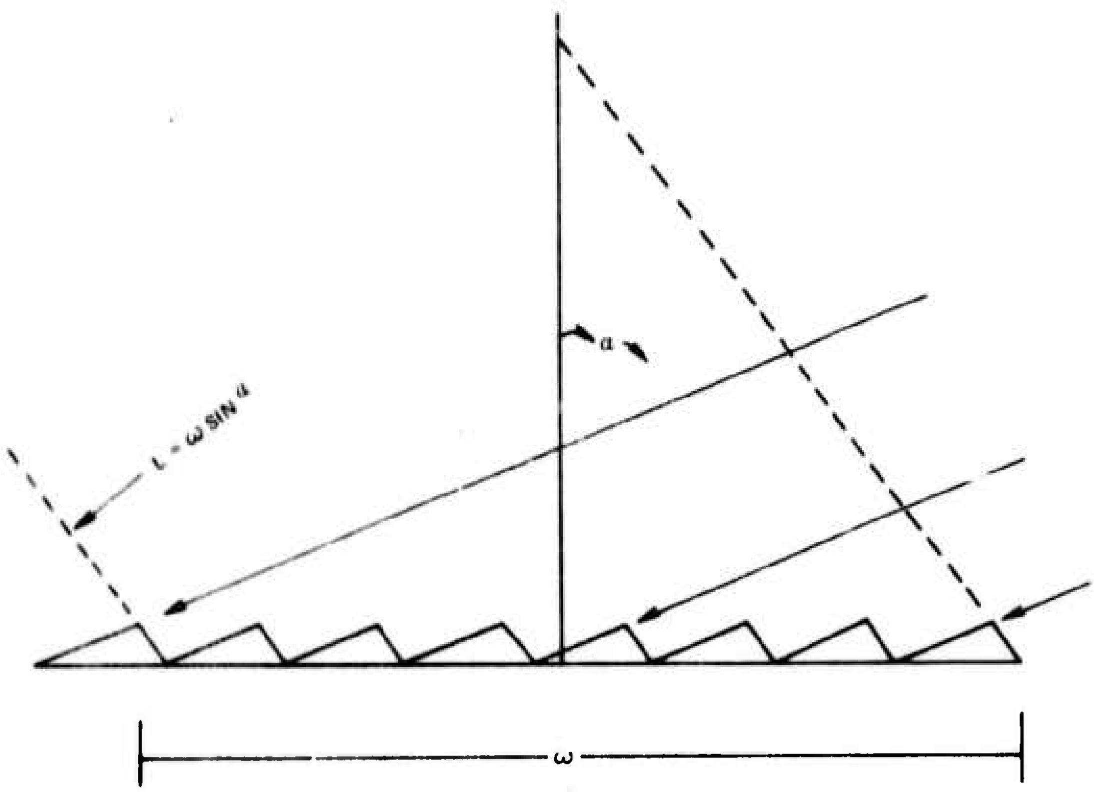

$$\Delta\tau = \frac{2L}{C} = \frac{2\omega \sin \alpha}{C}$$

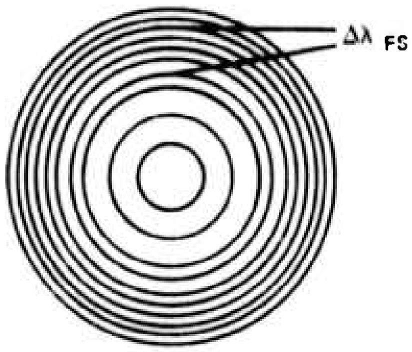

FRINGE PATTERN FROM
FABRY PEROT FILTER

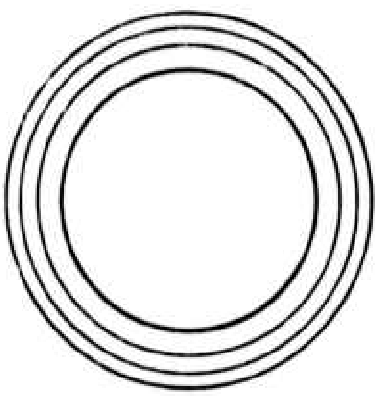

ONE FREE SPECTRAL RANGE

MULTIZONE DISK

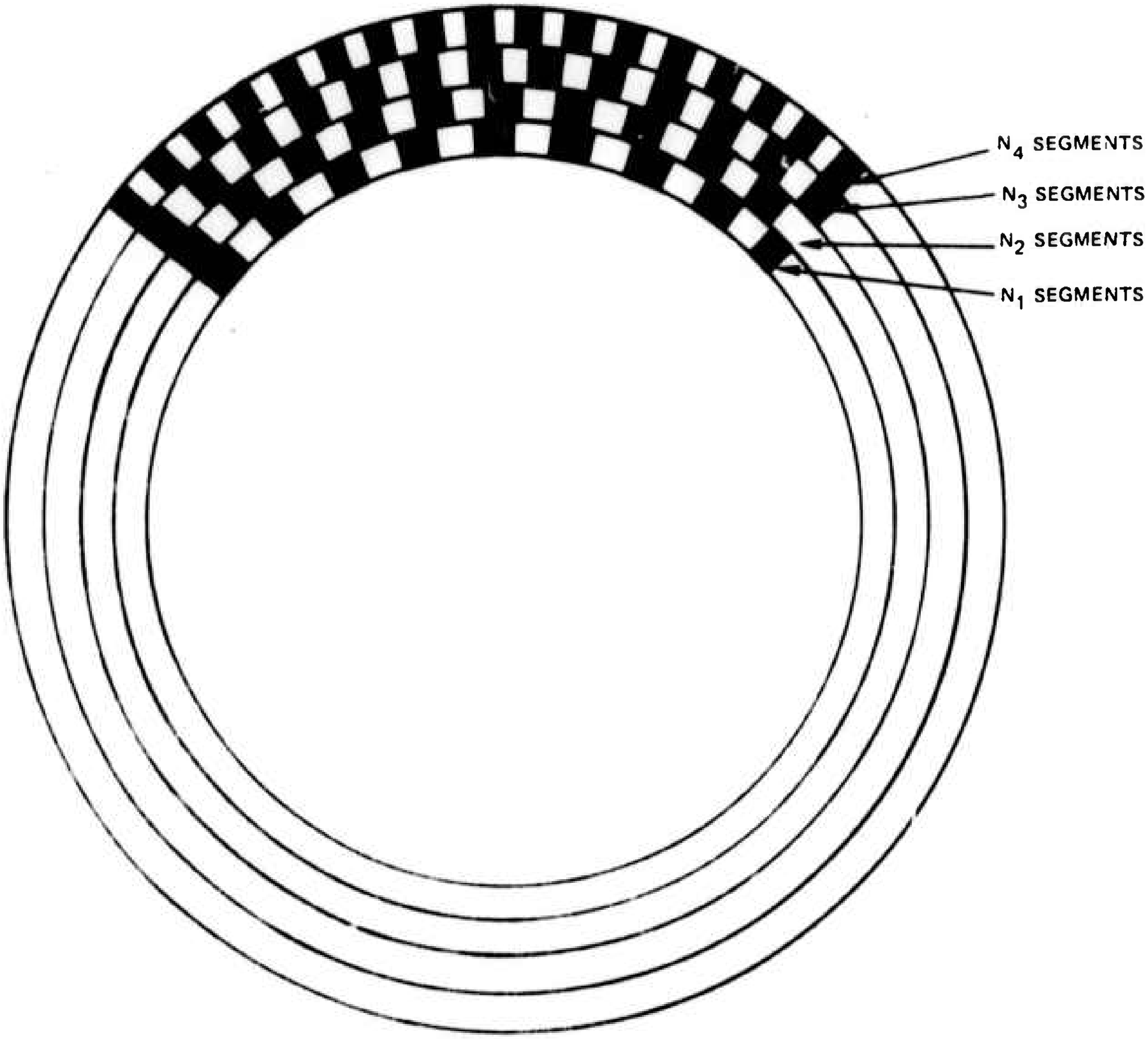

HETERODYNING OF INDIVIDUAL COMPONENTS OF LINE SPECTRUM

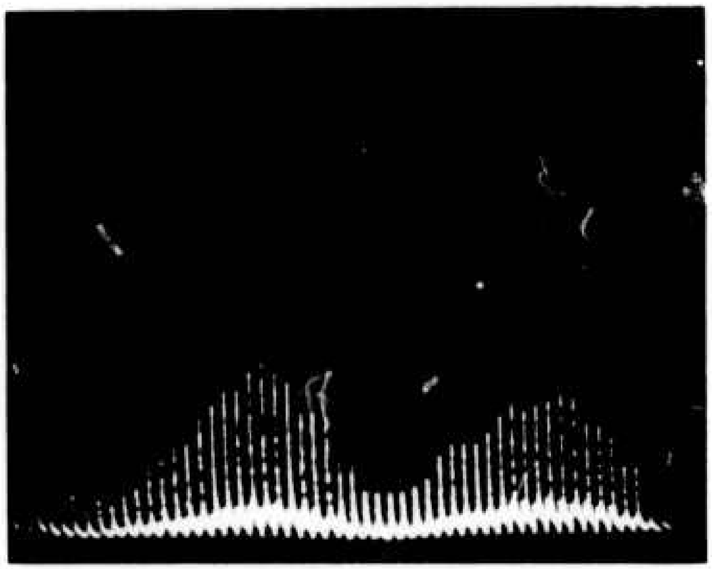

SINGLE MIRROR TARGET

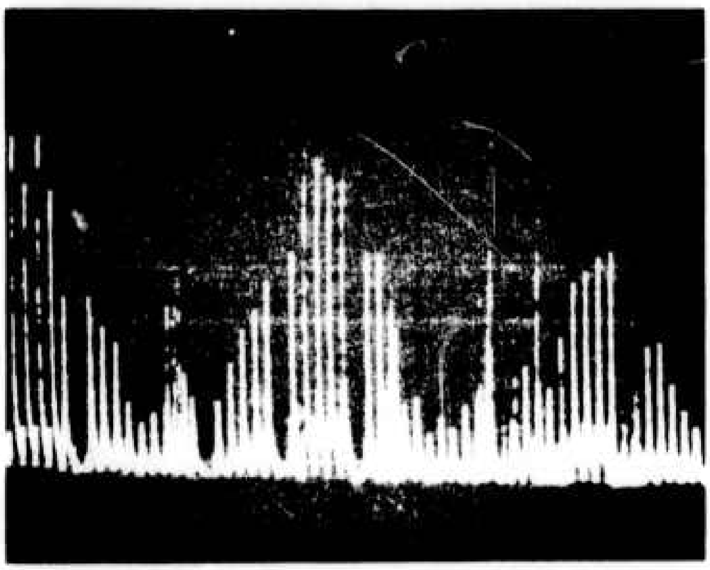

DOUBLE MIRROR TARGET

MULTIPLEXED GRATING SPECTROMETER

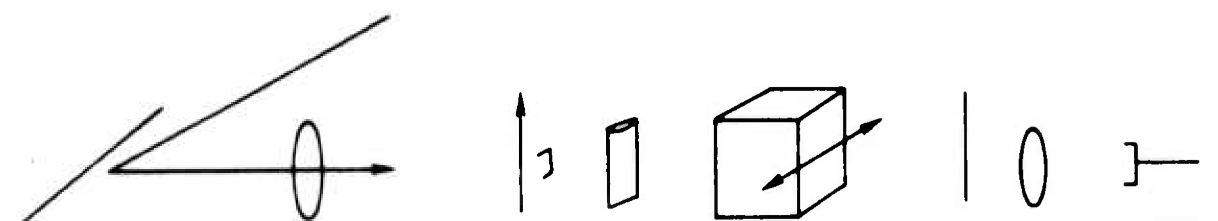

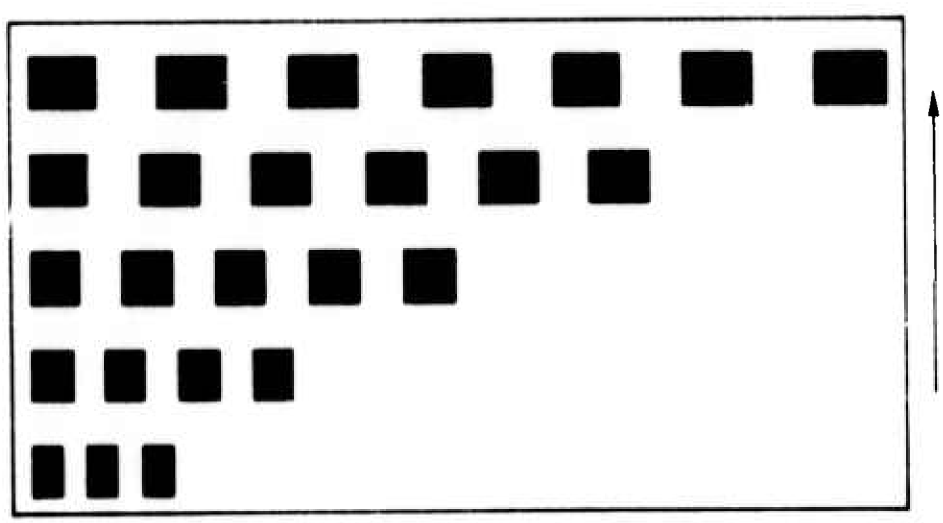

MASK (SCHEMATIC)